

## Structure-Dependent Kinetics for Synthesis and Decomposition of Formate Species over Cu(111) and Cu(110) Model Catalysts

Haruhisa Nakano,<sup>†</sup> Isao Nakamura,<sup>†</sup> Tadahiro Fujitani,<sup>‡</sup> and Junji Nakamura<sup>\*,†</sup>

*Institute of Materials Science, University of Tsukuba, Tsukuba, Ibaraki 305-8573, Japan, and National Institute for Resources and Environment, Tsukuba, Ibaraki 305-8569, Japan*

*Received: July 25, 2000; In Final Form: November 1, 2000*

The kinetics and mechanism of formate synthesis by hydrogenation of CO<sub>2</sub> (CO<sub>2</sub> + 1/2H<sub>2</sub> → HCOO<sub>a</sub>) and the formate decomposition into CO<sub>2</sub> and H<sub>2</sub> (HCOO<sub>a</sub> → CO<sub>2</sub> + 1/2H<sub>2</sub>) over Cu(111) and Cu(110) surfaces were studied by in-situ infrared reflection–absorption spectroscopy (IRAS) using a high-pressure reactor (~1 atm). The reaction rates and the apparent activation energy of the formate synthesis were measured for Cu(111) and Cu(110), indicating that the formate synthesis on Cu was found to be structure-insensitive. The pressure dependence of CO<sub>2</sub> and H<sub>2</sub> on the initial formation rate of formate suggested an Eley–Rideal type mechanism, in which a gaseous CO<sub>2</sub> molecule directly reacts with an adsorbed hydrogen atom on Cu. This is analogous to the well-known mechanism of formate synthesis by organometallic catalysts, in which CO<sub>2</sub> is inserted into a Cu–hydride bond. The reaction rates and the activation energy of the decomposition were measured for Cu(111) and Cu(110). It was found that the formate decomposition on Cu was structure-sensitive in contrast to the formate synthesis. The promotional effect of coexisting H<sub>2</sub> upon the rate of formate decomposition by 17 times at maximum was incidentally found only on Cu(111). Interestingly, the increase in the decomposition rate was due to an increase in the preexponential factor of the rate constant for the formate decomposition with the activation energy being constant. Furthermore, the decomposition kinetics of the formate prepared by adsorption of formic acid on O/Cu(111) was identical with the H<sub>2</sub>-promoted decomposition kinetics of the synthesized formate. The difference in the decomposition kinetics was ascribed to the ordered structure of formate based on the previous STM results, in which a chainlike structure of formate was observed for the synthesized formate, whereas no formate chain was observed for the formate prepared by adsorption of formic acid on O/Cu(111). The unique character of both the decomposition kinetics and the structure of formate observed only for Cu(111) was discussed from the viewpoint of the mass transport of copper atoms creating added formate chains.

### 1. Introduction

A surface science approach is available for studying the mechanism and kinetics of catalysis on solid surfaces from both macroscopic and microscopic viewpoints. In conjunction with industrial catalysts, the catalytic reactions should be examined under industrial conditions of 1 ~ 100 atm using a high-pressure reactor. The Somorjai group originally developed high-pressure studies in surface science to measure catalytic kinetics on well-defined surfaces, for example, hydrogenolysis and isomerization of hydrocarbons on Pt surfaces and ammonia synthesis on iron surfaces.<sup>1</sup> Several research groups have since measured the kinetics of major industrial catalytic reactions, such as methanation, Fischer–Tropsch synthesis, methanol synthesis, ethylene epoxidation, CO oxidation, the water-gas shift reaction and so on.<sup>2</sup> Although the surface science approach using a high pressure reactor has the potential for clarifying the detailed mechanism of the catalytic reactions at an atomic level, further studies have not been fully done. That is, one can further look into the microscopic mechanism, the nature of the active site, and the kinetics features using a variety of modern surface science

techniques, if a catalyst model can once be established on a single-crystal surface.

We have studied the kinetics and mechanism of methanol synthesis from CO<sub>2</sub> and H<sub>2</sub> on Cu model catalysts by surface science techniques using high-pressure reactors (1~18 atm),<sup>3–14</sup> while studying methanol synthesis over Cu–ZnO based powder catalysts.<sup>15–18</sup> We found that a Zn-deposited Cu(111) surface could be regarded as a good model of Cu/ZnO powder catalysts in terms of the turnover frequency of methanol production and the apparent activation energy. STM studies showed that the deposited Zn created a Cu–Zn active site on Cu(111), where Zn atoms were substituted for Cu atoms.<sup>13,19</sup> The assigned role of the Cu–Zn site in the reaction mechanism was to promote the hydrogenation of formate (HCOO) to methoxy (H<sub>3</sub>CO) species. Surface Cu atoms are also necessary for several hydrogenation steps such as formate synthesis from CO<sub>2</sub> and H<sub>2</sub>. That is, the Cu–Zn site and Cu atoms cooperate to catalyze methanol synthesis. We then tried to describe the mechanism of methanol synthesis on the Zn/Cu(111) model catalyst by the kinetics of the constituent elementary steps. The kinetic measurement of formate synthesis (CO<sub>2</sub> + 1/2H<sub>2</sub> → HCOO<sub>a</sub>) was first carried out on Zn/Cu(111) and clean Cu(111) surfaces at atmospheric pressure. During XPS and STM studies of formate, various interesting phenomena were observed regarding the kinetics of the synthesis and the decomposition of formate

\* Corresponding author. Fax: (+ 81) 298 557440, Tel: (+ 81) 298 535279, E-mail: nakamura@ims.tsukuba.ac.jp

<sup>†</sup> University of Tsukuba.

<sup>‡</sup> National Institute for Resources and Environment.

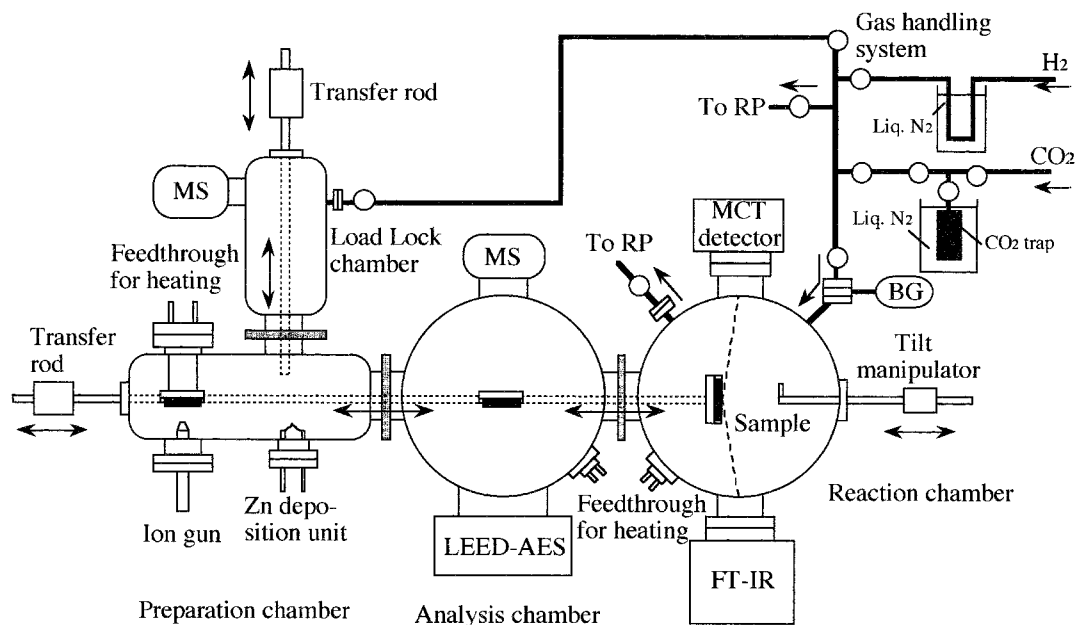


**Figure 1.** Schematic diagram of an IRAS apparatus equipped with a high-pressure reactor.

as well as the ordered structure.<sup>6,10,13,19</sup> Chainlike and non chainlike structures of formate were seen on Cu(111) depending on the preparation method.<sup>13,19</sup> Also, the decomposition kinetics of formate depended on the preparation method or the presence of hydrogen. Because of the very unique character and the importance of formate on Cu as a reaction intermediate in methanol synthesis, we concentrated on the systematic study of the synthesis and decomposition of formate on Cu(111) and Cu(110) as well as on a Cu/SiO<sub>2</sub> catalyst. We report here the characteristic kinetics for the synthesis and decomposition of formate on Cu(111) and Cu(110) in relation to adsorption structure.

The structure and the kinetic behavior of formate have been widely studied by surface science techniques.<sup>19–25</sup> On single-crystal Cu surfaces, formate is known to adsorb in a bridging bidentate form with two oxygen atoms bound to Cu atoms by IRAS, HREELS, and EXAFS studies.<sup>26–29</sup> The local registry of formate on Cu(111) has been recently determined by normal incidence X-ray standing wavefield absorption (NIXSW) in which the oxygen atoms are located on atop sites.<sup>30</sup> The adsorption site is identical to that reported for formate on Cu(110) and Cu(100).<sup>31,32</sup> STM studies showed that exposure of O/Cu(110) to formic acid resulted in the formation of  $c(2 \times 2)$  and  $(3 \times 1)$  formate structures depending on the oxygen coverage,<sup>25</sup> where the formate species studied is mostly prepared by adsorption of formic acid in UHV.

On the other hand, formate synthesis from CO<sub>2</sub> and H<sub>2</sub> was carried out on Cu single-crystal surfaces at high pressures (1–2 atm). Chorkendorff et al. have observed no difference in the decomposition kinetics on Cu(100) for the formate prepared by the adsorption of the formic acid in UHV and synthesized by hydrogenation of CO<sub>2</sub>.<sup>20</sup> However, our previous results indicated that the structure and the reactivity of formate prepared from formic acid on O/Cu(111) were quite different from those of the synthesized formate.<sup>13,19</sup> The difference in the kinetic feature originating from the ordered structures of formate was described in this paper.

We also describe the Eley–Rideal (E–R) type mechanism of formate synthesis strongly suggested by kinetic analysis. As far as we know, no E–R type mechanism has been reported for major industrial catalytic reactions over metal catalysts. Here,

we report the initial suggestion seen in the pressure dependence of H<sub>2</sub> and CO<sub>2</sub> upon formate synthesis on Cu(111). Further studies by a dynamic method and ab initio DFT calculations support the E–R mechanism, which will be reported soon.

## 2. Experimental Section

The experiments were conducted using UHV–infrared reflection absorption spectroscopy (IRAS) as shown in Figure 1. This apparatus is composed of four chambers: a load-lock chamber for changing the sample, a preparation chamber equipped with an ion gun for Ar<sup>+</sup> sputtering, an analysis chamber with facilities for low-energy electron diffraction (LEED), Auger electron spectroscopy (AES), and quadrupole mass spectroscopy (QMS), and a reaction chamber in which it is possible to carry out reactions at atmospheric pressure and take in-situ IRAS measurements during the reaction. The vibrational spectra in the range of 700–3000 cm<sup>-1</sup> were obtained at a resolution of 4 cm<sup>-1</sup> by 100 scans in a total measurement time of 30 s. An infrared spectrometer with a liquid nitrogen-cooled mercury–cadmium–telluride (MCT) detector was situated next to the reaction chamber. Each chamber is shut with a gate valve, and a sample is transferred using transfer rods. It is possible to transfer the sample without exposing it to the atmosphere.

The Cu(111) and Cu(110) disks (10 mm diameter, 2 mm thickness, and 5N purity) used in this study were polished only on one side. The accuracy of the crystal plane was less than one degree, and the surface roughness was within 0.03 μm. The sample was mounted along with two 0.25 mm diameter tungsten wires for resistive heating. The sample temperature was measured by a chromel–alumel thermocouple. The sample was cleaned by repeated Ar<sup>+</sup> sputtering at room temperature and 773 K and was then annealed at 773 K for 10–15 min. The cleanliness of the sample was evaluated by AES. A LEED pattern showed a clear (1 × 1) structure for Cu(111) and Cu(110). Because both CO<sub>2</sub> and H<sub>2</sub> have a low sticking probability on Cu surfaces at the temperatures used in this experiment, it is important to remove impurities such as CO and O<sub>2</sub> from the CO<sub>2</sub>/H<sub>2</sub> reaction gas. The CO<sub>2</sub> (99.9999% pure) was thus purified by freeze–pump–thaw cycles using liquid nitrogen. The H<sub>2</sub> (99.9999% pure) was purified by passing it through a tube cooled by liquid nitrogen.

The formate synthesis by the hydrogenation of CO<sub>2</sub> on the clean Cu(111) and Cu(110) surfaces was performed at 323–453 K, CO<sub>2</sub> = 76–380 Torr and H<sub>2</sub> = 10–380 Torr. After the sample temperature became constant at the reaction temperature, CO<sub>2</sub> and H<sub>2</sub> were subsequently introduced into the reaction chamber. The sample temperature was controlled within  $\pm 1$  K. In the experiment on formate synthesis, the reaction temperature was set at 323–353 K at which the thermal decomposition of the formate species was negligibly small.<sup>9,10</sup> A typical pressure condition of formate synthesis was CO<sub>2</sub>/H<sub>2</sub> = 380 Torr/380 Torr.

We have also studied the formate prepared by exposure to formic acid at 333 K in UHV. Formic acid was introduced onto the clean Cu(111), Cu(110), and oxygen-precovered and/or oxygen-free surfaces at  $1 \times 10^{-8} \sim 1 \times 10^{-6}$  Torr using a stainless steel leak valve. The formic acid (99%) was dried over copper sulfate anhydride and further purified by freeze–pump–thaw cycles prior to admission into the vacuum chamber. QMS was used to evaluate the purity of the formic acid.

It has been reported that the peak intensity of the  $\nu_s(\text{OCO})$  band observed at about 1340–1360 cm<sup>-1</sup> is proportional to the formate coverage ( $\Theta_{\text{HCOO}}$ ) on the copper surfaces.<sup>26</sup> We thus estimated formate coverage using the peak intensity of the  $\nu_s(\text{OCO})$ . In the XPS measurements of the same formate synthesis by the hydrogenation of CO<sub>2</sub>, the saturated formate coverage was determined to be 0.24 on Cu(111).<sup>6</sup> Also, in the previous STM results, a  $c(2 \times 4)$  structure as the most densely packed structure corresponding to  $\Theta_{\text{HCOO}} = 0.25$  was observed for the formate species synthesized from CO<sub>2</sub>/H<sub>2</sub> on Cu(111).<sup>13,19</sup> Furthermore, the saturated formate coverage on Cu(110) has been reported to be 0.25 based on a TPD analysis.<sup>26</sup> Thus, in this study, we adopted the saturation formate coverage ( $\Theta_{\text{HCOO}}^{\text{sat}}$ ) of 0.25 on both Cu(111) and Cu(110).

The isothermal decomposition of the formate species, prepared by the hydrogenation of CO<sub>2</sub> and adsorption of formic acid, was carried out by maintaining the sample at a constant temperature (358–403 K) in a vacuum. The decomposition rate was determined by the IRAS measurement of the formate coverage. After the decomposition of formate, the carbon residue was usually below the detection limit of AES.

### 3. Results

**3.1. Formate Synthesis.** Typical IRA spectra of formate synthesized on Cu(111) are shown in Figure 2, where the synthetic reaction was carried out at 353 K and 380 Torr CO<sub>2</sub>/380 Torr H<sub>2</sub>. The intensity of the peaks increased with increasing exposure to CO<sub>2</sub> and H<sub>2</sub>. However, no significant peak shifts were observed upon increasing the exposure. The peak positions were in good agreement with those reported for bridging bidentate formate species on Cu surfaces as shown in Table 1. That is, the peaks at 1354, 2850, and 2930 cm<sup>-1</sup> were assigned to the symmetric OCO stretching band ( $\nu_s(\text{OCO})$ ), the CH

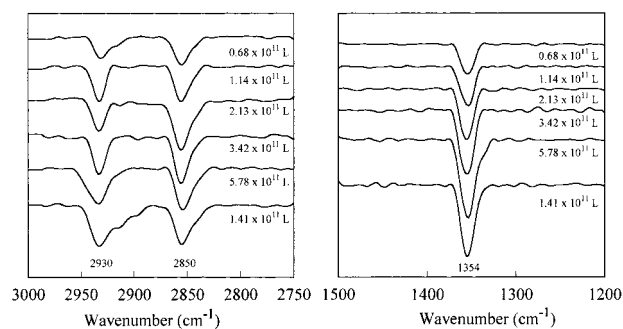


**Figure 2.** IRA spectra of formate species on Cu(111) synthesized by CO<sub>2</sub> hydrogenation (CO<sub>2</sub>/H<sub>2</sub> = 1, 760 Torr) at 353 K.

stretching band ( $\nu(\text{CH})$ ) and the combination band of the asymmetric OCO stretching and the in-plane CH bending modes, respectively. No other surface species were detected on the postreaction surfaces by AES.

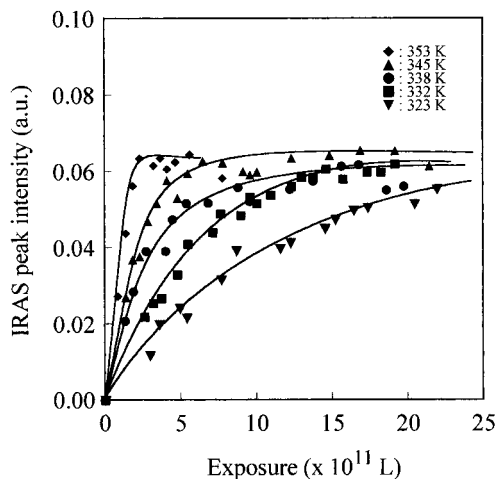
To elucidate the kinetics of formate synthesis, the buildup of formate was repeatedly measured at 333–353 K, at which the decomposition of formate was neglected on Cu(111). Figure 3 shows the peak intensity at 1353 cm<sup>-1</sup> as a function of total exposure of CO<sub>2</sub> and H<sub>2</sub>. These can be regarded as buildup curves because the peak intensity of  $\nu_s(\text{OCO})$  at 1350 cm<sup>-1</sup> is known to be proportional to the formate coverage.<sup>26</sup> The saturated coverage was identical regardless of the reaction temperature. In both XPS and STM studies,<sup>6,13,19</sup> the saturated formate coverage was determined to be  $\Theta_{\text{HCOO}} = 0.25$  under the same reaction conditions, where  $\Theta = 1$  corresponds to the number of Cu atoms on Cu(111),  $1.77 \times 10^{15}$  atoms cm<sup>-2</sup>. The initial formation rate of formate was thus obtained by the slope at zero formate coverage in Figure 3, for example,  $9.09 \times 10^{-4}$  molecules site<sup>-1</sup> sec<sup>-1</sup> at 353 K.

Figure 4 shows Arrhenius plots of the initial formation rate derived from the data in Figure 3 as well as our previous data measured by XPS and IRAS on Cu(111) and Cu(110).<sup>6,7</sup> It is shown that the formation rates on Cu(111) measured in this study are in agreement with those on Cu(111) measured by XPS within experimental error. The activation energy and the preexponential factor of the rate constant on Cu(111) were determined to be  $56.6 \pm 4.8$  kJ mol<sup>-1</sup> and  $2.27 \times 10^5$  molecules site<sup>-1</sup> sec<sup>-1</sup>, respectively. Those values measured by IRAS were comparable with those measured by XPS for the same Cu(111) sample, that is,  $54.6 \pm 5.9$  kJ mol<sup>-1</sup> and  $7.92 \times 10^4$  molecules site<sup>-1</sup> sec<sup>-1</sup>. Note that no significant difference in the kinetics of formate synthesis was observed among Cu(111), Cu(110), and Cu(100) as has already been reported,<sup>6,7,20</sup> indicating a structure-insensitive reaction. That is, the activation energies on Cu(110) and Cu(100)<sup>20</sup> have been reported to be  $59.8 \pm 4.1$  and  $55.6 \pm 8.0$  kJ mol<sup>-1</sup>, respectively. The absolute TOF (turnover frequencies) values were also close to each other.

Figures 5a and 5b show the pressure dependence of H<sub>2</sub> and CO<sub>2</sub> upon the initial formation rate of formate on Cu(111) at

**TABLE 1: Vibrational Frequencies (cm<sup>-1</sup>) for the Formate Species on Cu Single Crystals**

	$\nu_s(\text{OCO})$	$\nu(\text{CH})$	$\nu_{\text{comb}}$	preparation of formate	technique	ref
Cu(111)	1352–1354	2855	2932	CO <sub>2</sub> + H <sub>2</sub>	IRAS	[7]
Cu(111)	1342–1360	2850	2922	HCOOH	IRAS	This work
Cu(110)	1352–1362	2846–2850	2922–2928	CO <sub>2</sub> + H <sub>2</sub>	IRAS	[7]
Cu(110)	1352–1362	2846–2848	2922–2928	HCOOH	IRAS	This work
Cu(110)	1360	2920, 2960	-	H <sub>2</sub> CO, CH <sub>3</sub> OCHO	EELS	[27]
Cu(110)	1355	2848	2930	HCOOH	IRAS	[45]
Cu(110)	1348–1358	2891–2900	2946–2955	HCOOH	IRAS	[26]
Cu(100)	1325	2870	2930	HCOOH	HREELS	[28]
Cu(100)	1331	2840, 2910	-	HCOOH	HREELS	[44]
Cu(100)	1330	2879	-	CO <sub>2</sub> + H <sub>2</sub>	HREELS	[20]



**Figure 3.** Peak intensity at 1535  $\text{cm}^{-1}$  for formate species on Cu(111) as a function of exposure to  $\text{CO}_2$  and  $\text{H}_2$  ( $\text{CO}_2/\text{H}_2 = 1$  760 Torr).

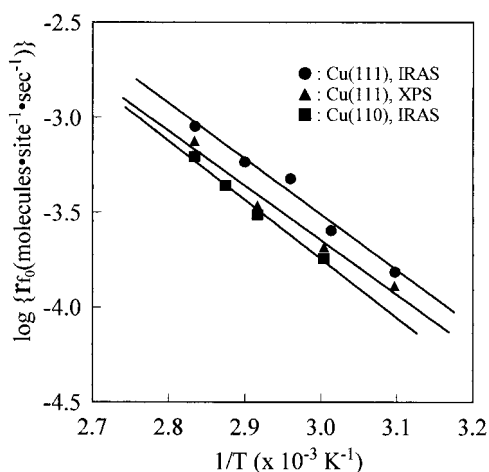


**Figure 4.** Arrhenius plots for the initial formation rates of formate species on Cu(111) (●: IRAS, ▲: XPS<sup>6</sup>) and Cu(110) (■: IRAS<sup>7</sup>).

**TABLE 2: Preexponential Factor and Activation Energy of Elementary Steps**

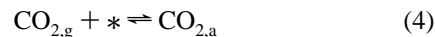
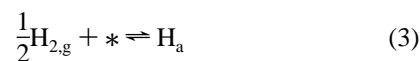
	preexponential factor ( $\text{cm}^2/\text{s}$ )	activation energy (kJ/mol)	ref
$\text{H}_2 + 2* \rightarrow 2\text{H}_a$	$k_1$	$10^{0.03}$	Cu(110) [33]
$2\text{H}_a \rightarrow \text{H}_2 + 2*$	$k_{-1}$	$3.4 \times 10^{-4}$	Cu(111) [34]
$\text{CO}_{2a} \rightarrow \text{CO}_2 + *$	$k_{-2}$	$10^{15}$	Cu(100) [20, 35]

333, 343, and 353 K. The  $\text{CO}_2$  (or  $\text{H}_2$ ) pressure was fixed at 380 Torr, whereas the  $\text{H}_2$  (or  $\text{CO}_2$ ) pressure was varied from 10 to 380 Torr. As for the  $\text{H}_2$  pressure dependence in Figure 5a, the increase in  $r_{f0}$  with  $\text{H}_2$  pressure became small at higher  $\text{H}_2$  pressures. On the other hand, the formation rate increased linearly with  $\text{CO}_2$  pressure as shown in Figure 5b.

The saturating behavior seen in Figure 5a is probably due to the coverage of hydrogen atoms, inhibiting surface reactions on the bare copper surface. We thus estimated the equilibrium coverage of  $\text{H}_a$  or  $\text{CO}_{2a}$  under the cited reaction conditions using kinetic data measured by surface science techniques summarized in Table 2. The coverage of  $\text{H}_a$  and  $\text{CO}_{2a}$  is shown in Figure 6 as a function of  $\text{H}_2$  and  $\text{CO}_2$  pressures, respectively. The equilibrium coverage of  $\text{H}_a$  at 343 K and 200 Torr  $\text{H}_2$  was calculated to be 0.52, whereas the  $\text{CO}_{2a}$  coverage was found to be very small ( $10^{-4}$ ) at 380 Torr  $\text{CO}_2$ . It is seen in Figure 5a that  $r_{f0}$  comes to saturation at 200 Torr  $\text{H}_2$  and 343 K. The hydrogen coverage is thus responsible for the nonlinear behavior shown in Figure 5a. We thus tried to analyze the kinetics of

the pressure dependencies as described in the following section.

Taylor et al.<sup>20</sup> have reported the kinetic analysis of the formate synthesis on Cu(100) assuming a Langmuir–Hinshelwood mechanism (L–H mechanism). We first analyze the kinetics of our data on Cu(111) assuming the L–H mechanism and the following elementary reaction steps.



Here, \* and subscript a stand for a vacant site and an adsorbed state, respectively, and the decomposition of formate, or the reverse reaction of eq 5, is neglected at the cited low temperatures in our experiments. One can thus obtain the following equations.

$$\Theta_{\text{H}} = \frac{k_1}{k_{-1}} P_{\text{H}_2}^{1/2} \Theta_* \quad (6)$$

$$\Theta_{\text{CO}_2} = \frac{k_2}{k_{-2}} P_{\text{CO}_2} \Theta_* \quad (7)$$

$$r_f = k_3 \Theta_{\text{H}} \Theta_{\text{CO}_2} \quad (8)$$

Here,  $k_1$  and  $k_{-1}$  are the rate constants of step 3 and the reverse step (3), respectively,  $k_2$  and  $k_{-2}$  are those for step 4 and the reverse step 4, respectively, and  $k_3$  is that for step 5. The formate species is assumed to occupy two copper atoms because it is known to adsorb in the bridging bidentate state.  $\Theta_{\text{CO}_2}$  is also neglected in the estimation of  $\Theta_*$  because it is very small as shown in Figure 6.  $\Theta_*$  is then expressed by the following equation.

$$\Theta_{\text{CO}_2} \approx 0$$

$$\Theta_* = 1 - \Theta_{\text{H}} - 2\Theta_{\text{HCOO}} \quad (9)$$

From eqs 6–9, the following equations are obtained.

$$\Theta_{\text{H}} = \frac{k_1}{k_{-1}} P_{\text{H}_2}^{1/2} \frac{1 - 2\Theta_{\text{HCOO}}}{1 + \frac{k_1}{k_{-1}} P_{\text{H}_2}^{1/2}} \quad (10)$$

$$\Theta_{\text{CO}_2} = \frac{k_2}{k_{-2}} P_{\text{CO}_2} \frac{1 - 2\Theta_{\text{HCOO}}}{1 + \frac{k_1}{k_{-1}} P_{\text{H}_2}^{1/2}} \quad (11)$$

$$r_f = \frac{k_1 k_2 k_3}{k_{-1} k_{-2}} P_{\text{H}_2}^{1/2} P_{\text{CO}_2} \frac{(1 - 2\Theta_{\text{HCOO}})^2}{\left(1 + \frac{k_1}{k_{-1}} P_{\text{H}_2}^{1/2}\right)^2} \quad (12)$$

At  $\Theta_{\text{HCOO}} = 0$

$$r_{f0} = \frac{k_1 k_2 k_3}{k_{-1} k_{-2}} P_{\text{H}_2}^{1/2} P_{\text{CO}_2} \frac{1}{\left(1 + \frac{k_1}{k_{-1}} P_{\text{H}_2}^{1/2}\right)^2} \quad (13)$$

The applicability of eq 13 was experimentally evaluated by the pressure dependence of the initial formation rate. Figures 7a and 7b show calculated (solid line) and experimental (plots)  $r_{f0}$

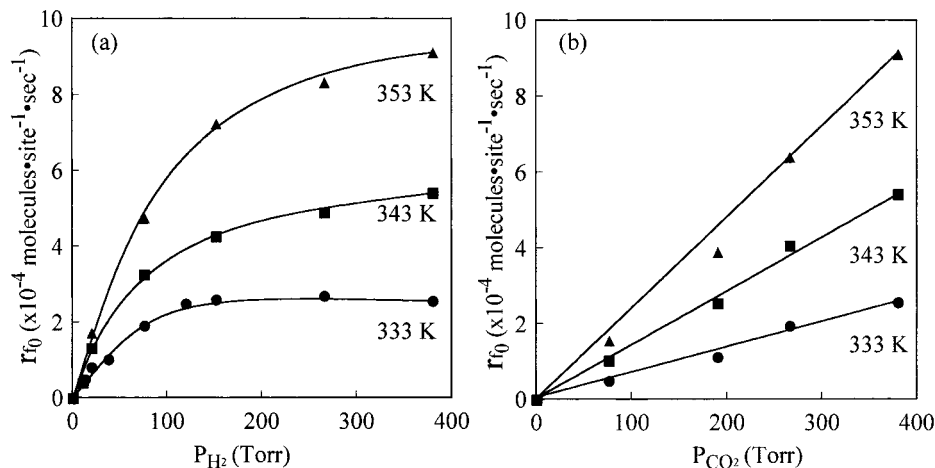


**Figure 5.** Dependence of the initial formation rate of formate on (a)  $H_2$  pressure dependence at  $P_{CO_2} = 380$  Torr (b)  $CO_2$  pressure dependence at  $P_{H_2} = 380$  Torr.

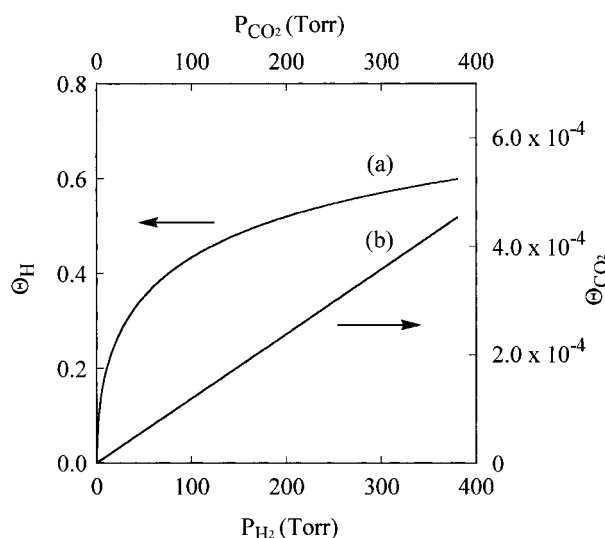


**Figure 6.** Equilibrium coverage of (a)  $H_a$  and (b)  $CO_{2,a}$  at 343 K.

for the dependences of  $H_2$  and  $CO_2$  pressures. In the calculation of  $r_{f0}$ , literature values of  $k_1$ ,  $k_{-1}$  and  $k_{-2}$ <sup>33–35</sup> were used, and  $k_2$  was calculated assuming that the sticking probability of  $CO_2$  was unity. The value of  $k_3$  in eq 13 was determined from the measured  $r_{f0}$  at  $CO_2/H_2 = 380$  Torr/380 Torr using  $k_1$ ,  $k_{-1}$ ,  $k_2$ , and  $k_{-2}$ . Finally, the calculated  $r_{f0}$  (solid line) was thus obtained at various  $H_2$  pressures using eq 13. As shown in Figure 7, the measured  $r_{f0}$  at different  $H_2$  pressures were in disagreement with the calculated  $r_{f0}$ , although good agreement between the calculation and measurement of  $r_{f0}$  was obtained for  $CO_2$  pressure dependence.

We then tried to calculate  $r_{f0}$  assuming an E–R type mechanism in which a gaseous  $CO_2$  molecule directly reacts with an adsorbed hydrogen atom on Cu(111). The reaction is expressed by the following equations.



The formation rate of formate is then expressed by the following equation.

$$\begin{aligned} r'_f &= k_3 P_{CO_2} \Theta_{H_a} \\ &= \frac{k_1 k_3'}{k_{-1}} P_{H_2}^{1/2} P_{CO_2} \frac{1 - 2\Theta_{HCOO}}{1 + \frac{k_1}{k_{-1}} P_{H_2}^{1/2}} \quad (16) \end{aligned}$$

At  $\Theta_{HCOO} = 0$

$$r'_{f0} = \frac{k_1 k_3'}{k_{-1}} P_{H_2}^{1/2} P_{CO_2} \frac{1}{1 + \frac{k_1}{k_{-1}} P_{H_2}^{1/2}} \quad (17)$$

The major difference between eqs 13 and 17 is the order in  $(1 + (k_1/k_{-1})P_{H_2}^{1/2})$ . In the L–H mechanism, the adsorbed hydrogen hinders both  $H_2$  dissociative adsorption and  $CO_2$  adsorption so that the order is second in  $(1 + (k_1/k_{-1})P_{H_2}^{1/2})$ . Similarly to the calculation of  $k_3$ ,  $k_3'$  was calculated from an experimentally measured  $r_{f0}$  under the pressure condition of  $CO_2/H_2 = 380$  Torr/380 Torr. As shown in Figure 7, the experimental data were in fairly good agreement with the calculated  $r_{f0}'$  (broken line) at both different  $H_2$  and  $CO_2$  pressures. The kinetic analysis of formate synthesis thus suggested the E–R type mechanism, which will be further discussed in section 4.1.

**3.2. Formate Decomposition.** The isothermal decomposition of formate on Cu(111) was carried out in UHV at 358–403 K. The formate was synthesized from  $CO_2$  and  $H_2$  at 343 K, and the initial coverage was 0.25. The following rate equation can be obtained for the formate decomposition if the decomposition is first order in formate coverage.

$$r_d = -\frac{d\Theta_{HCOO}}{dt} = k_d \Theta_{HCOO} \quad (18)$$

$$\log \Theta_{HCOO} = -k_d t + \log \Theta_{HCOO}^{sat} \quad (19)$$

Here,  $\Theta_{HCOO}^{sat}$  is the saturation coverage of formate (0.25). Figure 8 shows  $\log \Theta_{HCOO}$  as a function of reaction time. The linearity indicates that the decomposition rate is first order in formate coverage in agreement with the literature data on Cu(110) measured by TPD.<sup>36</sup> The rate constant  $k_d$  was then obtained from the slope. At 373 K, for example, the rate constant was  $1.50 \times 10^{-4} \text{ sec}^{-1}$ .

Figure 9 shows Arrhenius plots of the initial decomposition rate ( $r_{d0}$ ) derived from the data shown in Figure 8, as well as our previous data for Cu(110)<sup>7</sup> and literature data of Cu(100).<sup>20</sup>

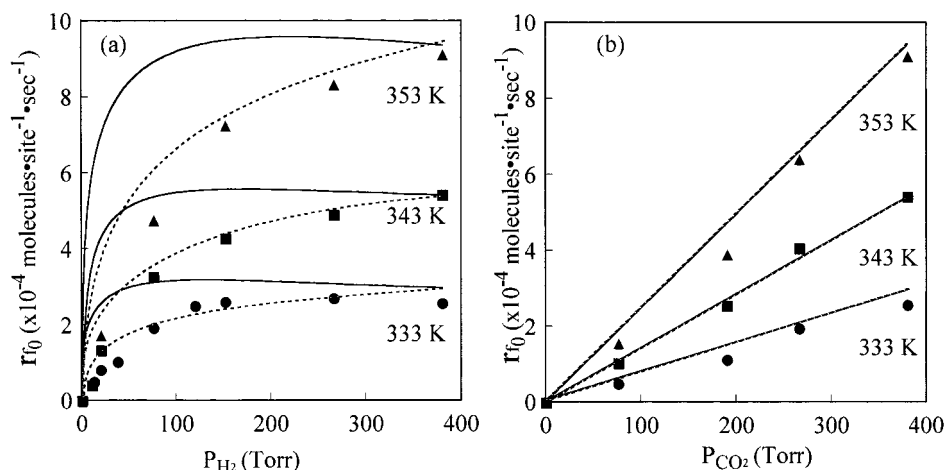


**Figure 7.** Dependence of the initial formation rate of formate on (a)  $H_2$  pressure ( $P_{CO_2} = 380$  Torr constant) (b)  $CO_2$  pressure ( $P_{H_2} = 380$  Torr constant).  $\bullet$ ,  $\blacksquare$ ,  $\blacktriangle$ : experimental data, solid lines: calculation data assuming an L-H mechanism, dashed lines: calculation data assuming an E-R mechanism.

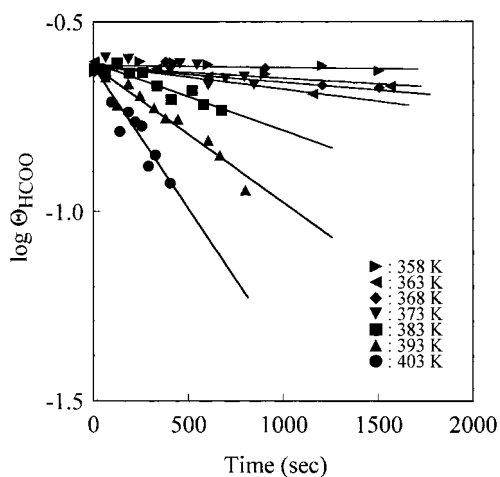


**Figure 8.** Logarithm of the formate coverage as a function of time in the decomposition of formate species synthesized by  $CO_2$  hydrogenation on Cu(111).

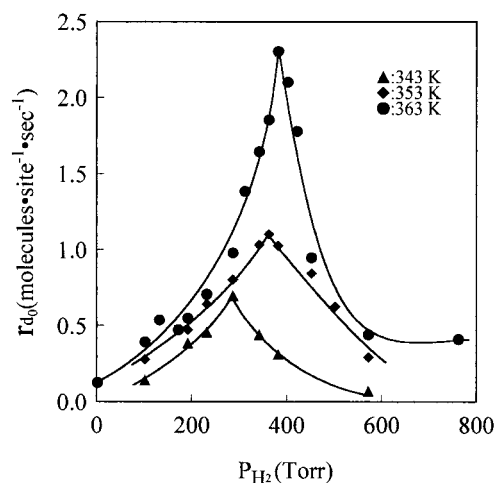


**Figure 10.** Dependence of the initial decomposition rates of the formate species on  $H_2$  pressure.

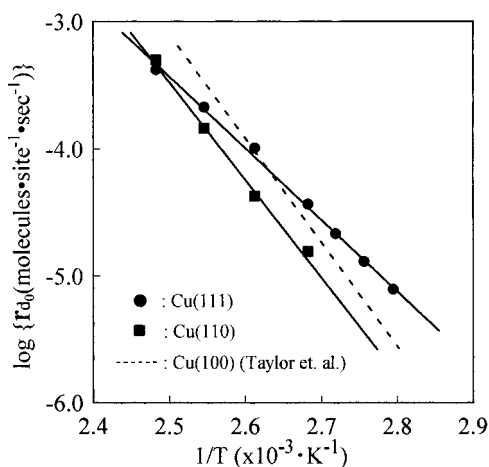


**Figure 9.** Arrhenius plots of the initial decomposition rate of formate species on Cu(111) ( $\bullet$ ), Cu(110) ( $\blacksquare$ ),<sup>7</sup> and Cu(100) (dashed line).<sup>20</sup>

Here, the initial rate was calculated at the saturation coverage of 0.25 using the rate constant. As shown in Figure 9, it was found that the activation energy was different depending on the orientation of the Cu surface. The activation energy and the preexponential factor of  $k_d$  were determined to be  $107.9 \pm 2.8$  kJ mol $^{-1}$  and  $1.87 \times 10^{11}$  sec $^{-1}$ , respectively, which are

comparable with those measured on Cu(111) by XPS.<sup>10</sup> The activation energies on Cu(110) ( $145.2 \pm 7.2$  kJ mol $^{-1}$ ) and on Cu(100) ( $155$  kJ mol $^{-1}$ ) are greater than that on Cu(111), showing that the decomposition of formate on Cu surfaces is structure-sensitive. This is in contrast to the structure-insensitive character of the formate synthesis, which is discussed in section 4.1.

We accidentally found that the decomposition rate of formate significantly varied in the presence of hydrogen. Figure 10 shows the dependence of the initial decomposition rate on  $H_2$  pressure at 343, 353, and 363 K. Interestingly, the decomposition rate steeply increased with  $H_2$  pressure and then sharply decreased. At 363 K, the maximum rate at 380 Torr was 17 times greater than that in the absence of  $H_2$ . We confirmed no production of formic acid by the hydrogenation of formate. The effect of hydrogen upon an increase in the decomposition rate was ascribed to the destruction of the formate chain by adsorbed hydrogen as discussed in 4.3. At high  $H_2$  pressure, coverage of hydrogen atoms will increase on the formate-covered Cu(111) surface, which probably hinders the decomposition of formate. The peaks seen in Figure 10 tend to be shifted to higher  $H_2$  pressures at higher temperatures, suggesting that the hydrogen equilibrium coverage controls the position of the peak maximum because higher  $H_2$  pressure is required at higher temperature to obtain a certain equilibrium hydrogen coverage. For example,

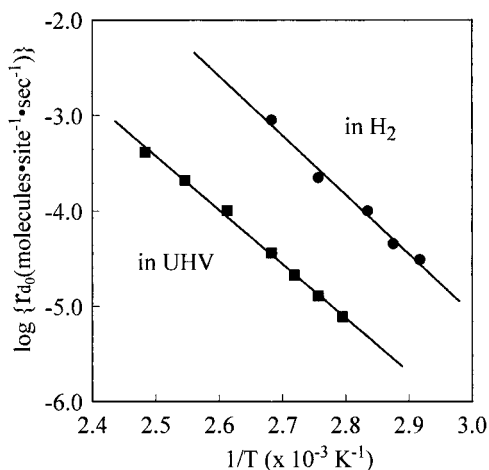


**Figure 11.** Arrhenius plots for the initial decomposition rate of the formate species on Cu(111). (●: decomposed in H<sub>2</sub> 380 Torr, ■: decomposed in a vacuum).

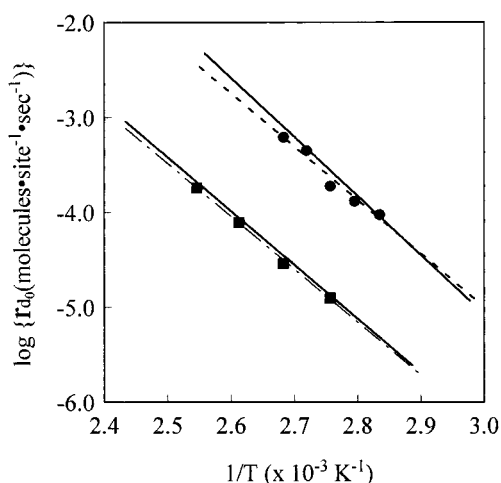


**Figure 12.** Arrhenius plots for the initial decomposition rate of the formate species on Cu(111). The formate prepared by adsorption of formic acid on Cu(111) (●) and O/Cu(111) (■) decomposed in a vacuum and the formate synthesized CO<sub>2</sub> and H<sub>2</sub> decomposed in a vacuum (long dashed line) and in H<sub>2</sub> 380 Torr (dashed line).

equilibrium coverage of hydrogen on Cu(111) in the absence of formate species can be estimated to be 0.54 at 380 Torr H<sub>2</sub> and 363 K.

We then compared the activation energies of the formate decomposition in UHV and in the presence of 380 Torr H<sub>2</sub>. Figure 11 shows the Arrhenius plots of the initial decomposition rate at  $\Theta_{\text{HCOO}} = 0.25$ . The activation energy of the decomposition in 380 Torr H<sub>2</sub> ( $118.4 \pm 7.7 \text{ kJ mol}^{-1}$ ) was found to agree with that in UHV ( $107.9 \pm 2.8 \text{ kJ mol}^{-1}$ ), although the decomposition rate was very different, indicating that only the preexponential factor of the rate constant was different. The preexponential factors were determined to be  $1.25 \times 10^{14}$  and  $1.87 \times 10^{11} \text{ sec}^{-1}$  for the decompositions in 380 Torr H<sub>2</sub> and in UHV, respectively. Very interestingly, as shown in Figure 12, the decomposition of the formate species prepared by adsorption of formic acid over an O<sub>a</sub>-preadsorbed Cu(111) ( $2\text{HCOOH} + \text{O}_a \rightarrow 2\text{HCOO}_a + \text{H}_2\text{O}$ ) in UHV showed the same kinetics as the decomposition kinetics of the synthesized formate in 380 Torr H<sub>2</sub>. On the other hand, the decomposition kinetics of the formate prepared by adsorption of formic acid on a clean Cu(111) was same as that in the absence of H<sub>2</sub> for the synthesized formate. In summary, the results described above indicate that two types of formate exist with different preex-

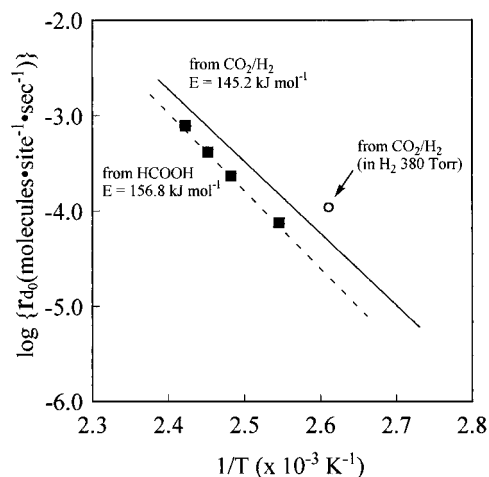
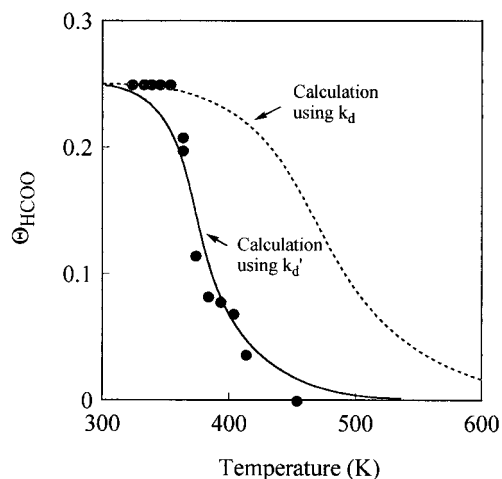


**Figure 13.** Arrhenius plots for the initial decomposition rate of the formate species on Cu(110). The synthesized formate species from CO<sub>2</sub> and H<sub>2</sub> were decomposed in a vacuum (solid line) and in 380 Torr H<sub>2</sub> 380 Torr (○). The formate prepared by adsorption of formic on a clean Cu(110) surface was decomposed in a vacuum (■, broken line).

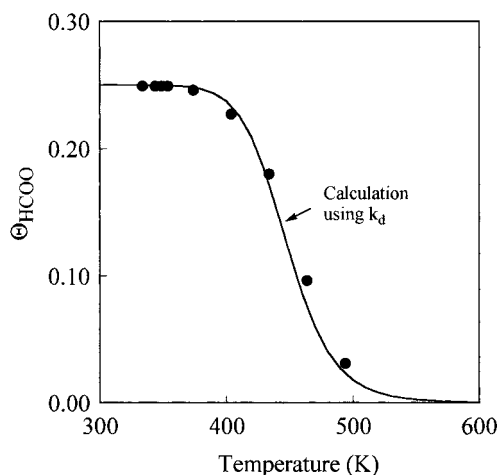
potential factors of the decomposition rate constant depending on the preparation method of the formate and the presence of H<sub>2</sub>. The reason for the difference was ascribed to the adsorption structure of formate on Cu(111) previously observed by STM as discussed in section 4.2, in which the OCO vibration of formate toward the surface was regarded to be responsible for the preexponential factor of the decomposition rate constant or the frequency factor. Similarly, difference in the decomposition rate of formate has been reported for Cu(110) with and without preadsorbed oxygen.<sup>23</sup>

Figure 13 shows Arrhenius plots of the initial decomposition rate of formate on Cu(110). The decomposition rate of the synthesized formate in H<sub>2</sub> 380 Torr at 383 K ( $1.01 \times 10^{-4}$  molecules site<sup>-1</sup> sec<sup>-1</sup>) was comparable with that in a vacuum at 383 K ( $4.35 \times 10^{-5}$  molecules site<sup>-1</sup> sec<sup>-1</sup>). In contrast to Cu(111), no significant promotion by H<sub>2</sub> in the decomposition kinetics was observed for the synthesized formate. The activation energy of the decomposition of the formate prepared from formic acid on a clean Cu(110) surface was determined to be  $156.8 \text{ kJ mol}^{-1}$ . The activation energy and the absolute decomposition rate were comparable with those for the synthesized formate. On Cu(110), no significant difference in the decomposition kinetics of formate was observed depending on the presence of H<sub>2</sub> and the preparation method. Possibly, the difference in the kinetics is due to the added formate chain suggested by the previous STM data as discussed in section 4.3.

**3.3. Equilibrium Formate Coverage.** Figure 14 shows the equilibrium coverage of formate on Cu(111) under hydrogenation of CO<sub>2</sub> at 380 Torr CO<sub>2</sub>/380 Torr H<sub>2</sub>. As shown by the plots, the measured formate coverage was saturated at  $\Theta_{\text{HCOO}} = 0.25$  up to 353 K. The coverage steeply decreased above 353 K and was below a detection limit at 453 K. The solid and broken lines are the calculated formate coverage based on the measured kinetics for the formate synthesis (3.1.) and the formate decomposition (3.2.) using  $k_d'$  and  $k_d$ , respectively, which are the rate constants of the formate decomposition measured in the presence of 380 Torr H<sub>2</sub> and in UHV. The calculated equilibrium coverage using  $k_d'$  is smaller than that calculated using  $k_d$  because the decomposition rate was much greater in the presence of H<sub>2</sub> compared to that in UHV as described in 3.2. The experimental data were in fairly good agreement with the calculated coverage using  $k_d'$ . That is, one



**Figure 14.** Equilibrium coverage of formate species on Cu(111) under hydrogenation of CO<sub>2</sub> at 380 Torr CO<sub>2</sub>/380 Torr H<sub>2</sub>. ●: experimental, dashed line; calculation using decomposition rate constant in UHV, solid line: calculation using decomposition rate constant in H<sub>2</sub> 380 Torr.



**Figure 15.** Equilibrium coverage of formate species on Cu(110) under hydrogenation of CO<sub>2</sub> at 380 Torr CO<sub>2</sub>/380 Torr H<sub>2</sub>. ●: experimental, solid line: calculation using decomposition rate constant in UHV.

should be careful of the effect of coexisting gases when discussing the microscopic kinetics of surface elementary steps. At a typical reaction temperature of 523 K for methanol synthesis, the formate coverage is as low as  $1.3 \times 10^{-3}$  in Figure 14. However, the coverage will be increased at higher pressures.

In comparison with Cu(111), the equilibrium formate coverage on Cu(110) is shown in Figure 15. The measured coverage was in good agreement with that calculated based on the kinetics of formate synthesis and formate decomposition shown in Figures 4 and 13. It was found that the equilibrium coverage on Cu(110) was much greater than that on Cu(111) at 400–500 K, which was mainly due to the absence of the promotion effect on the decomposition rate by H<sub>2</sub>. Thus, it is important to clarify that the promotion effect of H<sub>2</sub> on the decomposition should appear only for Cu(111). That is the same question raised regarding the results of Figures 11 and 13, which is discussed in section 4.3.

#### 4. Discussion

**4.1. Structure Sensitivity.** In organometallic chemistry, it is well-known that formate is synthesized by the reaction of CO<sub>2</sub> with transition metal complexes such as [HCuPPh<sub>3</sub>]<sub>6</sub>,<sup>37</sup> [Ph<sub>2</sub>P(CH<sub>2</sub>)<sub>2</sub>PPh<sub>2</sub>]<sub>2</sub>RhH,<sup>38</sup> or (PMePh<sub>2</sub>)<sub>3</sub>Cu(BH<sub>4</sub>).<sup>39</sup> Beguin et

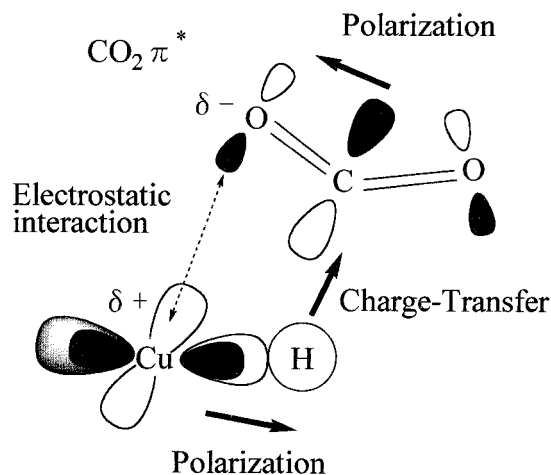


**Figure 16.** Model of CO<sub>2</sub> insertion into a Cu–H bond of CuH(PH<sub>3</sub>)<sub>2</sub> or CuH(PH<sub>3</sub>)<sub>3</sub> complex proposed by Sakaki et al.<sup>40</sup>

al.<sup>37</sup> have found that CO<sub>2</sub> inserts into a Cu–H bond in [HCuPPh<sub>3</sub>]<sub>6</sub>, leading to the formation of [Ph<sub>3</sub>P]<sub>2</sub>CuCOOH by IR. Sakaki et al.<sup>40,41</sup> carried out an ab initio MO study of the insertion of CO<sub>2</sub> into a metal-hydride bond of [RhH(PH<sub>3</sub>)<sub>3</sub>] and [CuH(PH<sub>3</sub>)<sub>3</sub>]. They have reported that the CO<sub>2</sub> insertion was significantly exothermic and that its activation barrier was estimated to be rather small (14.7 kJ mol<sup>-1</sup>), suggesting that the CO<sub>2</sub> insertion into the Cu(I)–H bond was facile. Figure 16 shows the model of the insertion of CO<sub>2</sub> into the Cu–H bond reported in ref 40, in which Sakaki et al. described that “the η<sup>1</sup>-C-coordinated CO<sub>2</sub> is significantly distorted, which pushes down the CO<sub>2</sub>π\* orbital energy.” As a result, “CO<sub>2</sub> interacts with the H ligand through the charge-transfer interaction from the H ligand to CO<sub>2</sub> and the electrostatic interaction between Cu<sup>δ+</sup> and O<sup>δ-</sup> atoms. Additionally, the charge-transfer interaction from O to Cu contributes to the Cu–O bond formation in the last stage of the reaction.” The proposed E–R type mechanism for the formate synthesis on Cu(111) based on the kinetic analysis here is analogous to the insertion of CO<sub>2</sub> into the Cu–H bond in the [HCuPPh<sub>3</sub>]<sub>6</sub> complex in terms of the direct reaction of CO<sub>2</sub> and the Cu–H bond without CO<sub>2</sub> adsorption on Cu. The E–R type mechanism may further explain the structure-insensitive character observed for the formate synthesis on Cu shown in Figure 4. That is, because the direct reaction of CO<sub>2</sub> with the Cu–H bond occurs at a local site on the Cu surface, the kinetic factors such as activation energy may be insensitive to the configuration of the surrounding Cu atoms. Very recently, we have obtained preliminary results to support the E–R type mechanism, in which the rate of the formate synthesis by the reaction of heated CO<sub>2</sub> molecules with a hydrogen-preadsorbed Cu(111) surface increased with increasing CO<sub>2</sub> gas temperature while maintaining the Cu(111) surface at room temperature. The results are in preparation for publication. We are continuing this kind of experiment by varying the surface temperature and the CO<sub>2</sub> pressure in order to obtain solid evidence for the E–R type mechanism.

In contrast to the formate synthesis, the formate decomposition on the Cu surfaces showed a structure-sensitive character as described in section 3.2. We propose a model to explain this unique character with respect to structure sensitivity as shown in Figure 17. The vibration of the OCO molecular plane in a bidentate formate toward the Cu surface is required in order to overcome the transition state (TS) for the formate decomposition. The surrounding Cu atom thus takes part in the decomposition process so that the position of the neighboring Cu atoms affects the kinetics of the decomposition, leading to the structure-

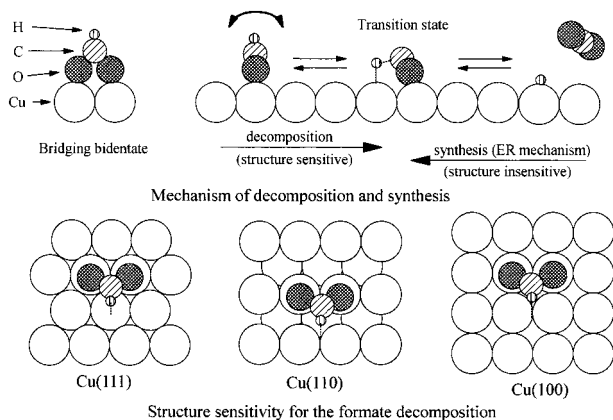


**Figure 17.** Model of formate chemistry on Cu.

sensitive character. We thus infer that the path in the reaction coordinate to overcome the barrier to the formate synthesis is structure-insensitive, whereas the path going through TS toward the decomposition is structure-sensitive. The difference in the activation energy for the decomposition may be related to the adsorption energy of the formate species, although the detailed microscopic mechanism is ambiguous.

**4.2. Kinetics Depending on the Ordered Structure of Formate.** As shown in Figure 12, the decomposition rate of formate prepared from formic acid on O/Cu(111) was greater than that for the formate synthesized from CO<sub>2</sub> and H<sub>2</sub>. Interestingly, the apparent activation energy for the decomposition in both cases was almost identical, whereas the preexponential factor of the rate constant was very different between those two formate species. These phenomena were also confirmed by our XPS studies.<sup>10</sup> We then studied the adsorption structure of formate by STM in order to examine the difference in the decomposition kinetics of formate.<sup>13,19</sup> It was found that the synthesized formate adsorbed in a chain structure with the distance to the nearest neighbor formate being twice that of the nearest neighbor Cu. Even at low formate coverage, a single formate chain was observed by STM, indicating that an anisotropic attractive interaction operated between the formate species. This further means that the attractive interaction should be quite strong and the barrier of diffusion is remarkably high. On the other hand, no chain structure was observed for the formate prepared from formic acid on O/Cu(111). However, (4 × 4) and (3 × 7/2) structures appeared, where the formate species adsorbed more dispersedly. The spacing between formate species was varied from four to three times that of the nearest neighbor Cu atoms in contrast to the synthesized formate with the spacing twice that of the nearest neighbor Cu atoms independent of formate coverage. It is possible that the decomposition of formate proceeds via the OCO plane vibration as shown in Figure 17, which has been proposed by Bowker et al. for acetate decomposition on Rh(111).<sup>46</sup> In this case, the frequency of the plane vibration should significantly influence the preexponential factor of the rate constant of the formate decomposition. The observed significant decrease in the preexponential factor with no variation in the activation energy is thus possibly due to the plane vibration of formate. That is, the OCO plane vibration may be hindered by the attractive interaction between the nearest neighbored formate species in a chain. Such an attractive interaction is absent between formate species prepared from formic acid. The difference in the adsorption structure thus reflects the reaction kinetics of the formate decomposition.

The difference in the adsorption structure depending on the

preparation method was suggested by the IRA spectra of formate. The peak position of  $\nu_s(\text{OCO})$  vibration for the formate on Cu(111) synthesized by CO<sub>2</sub> hydrogenation slightly shifted to high frequencies (2 cm<sup>-1</sup>, 1352 ~ 1354 cm<sup>-1</sup>) with increasing formate coverage. However, significant peak shifts of 18 cm<sup>-1</sup> (1342 ~ 1360 cm<sup>-1</sup>) were observed depending on formate coverage for the formate species prepared from formic acid and O/Cu(111). The difference in IRAS can be also explained by the adsorption structure of formate in the following. For the chain structure, the local environment of the formate does not change with formate coverage because the chain structure starts to grow at very low formate coverage. On the other hand, for the formate from formic acid on O/Cu(111), the distance to the nearest neighbor formate was continuously decreased with increasing formate coverage, leading to a continuous change in the local environment of formate. The repulsive force between formate species thus continuously varies as a function of the formate–formate distance or formate coverage, leading to the change in the IRA spectra of formate. The more interesting difference seen in IRAS was the sensitivity of IR peak intensity. In the XPS measurements of formate buildup, the saturated formate coverage was 0.25 and 0.33 for the formate synthesized from CO<sub>2</sub> and H<sub>2</sub> on Cu(111) and the formate prepared from formic acid on O/Cu(111), respectively. That is, both saturated coverages were not very different. In similar buildup measurements of formate by IRAS, however, the intensity of the IR peak for the synthesized formate at saturation was one-third of that for the saturated formate prepared from formic acid on O/Cu(111). The difference in the sensitivity was reproducibly observed. The decrease in intensity for the synthesized formate forming the formate chain was explained by the screening effect known in IRAS measurement in which closely located formate in a chain screens the neighboring dipole moment. In Figure 14, the equilibrium formate coverage below 360 K is consistent with the synthesis/decomposition kinetics using  $k_d$  (for the decomposition of the synthesized formate), whereas above 360 K the equilibrium coverage is in accordance with the kinetics using  $k_d'$  (for the decomposition of the formate prepared from formic acid as well as the decomposition of the synthesized formate in H<sub>2</sub>). Apparently, the equilibrium property seems to change at 360 K, which is probably due to a change in the structure of formate, i.e., chain and nonchain structures.

On Cu(110), no significant difference depending on the presence of H<sub>2</sub> or the preparation method of formate was observed in the decomposition kinetics as shown in Figures 13 and 15. The peak intensity of formate on Cu(110) was comparable with that for the formate prepared from formic acid on O/Cu(111), suggesting the absence of the screening effect. This is also supported by a peak shift of the  $\nu_s(\text{OCO})$  vibration (1352 ~ 1362 cm<sup>-1</sup>) at formate coverages between 0 and 0.25 for both formate species prepared from formic acid and synthesized by CO<sub>2</sub> hydrogenation on Cu(110). The peak shift of 10 cm<sup>-1</sup> has also been reported in the literature for formate species prepared from formic acid on Cu(110).<sup>26</sup> The absence of screening and the peak shift of the  $\nu_s(\text{OCO})$  vibration for formate on Cu(110) indicate the absence of the strong attractive interaction seen for the formate chain on Cu(111). However, Leibsle and Haq have reported a chainlike structure of formate on Cu(110).<sup>42,47,48</sup> We think that the interaction between formate in a chain is very different on Cu(111) and Cu(110).

**4.3. Possibility of Added Structure.** As described in sections 3.2 and 4.2, several unique features of the decomposition kinetics were observed only for Cu(111). Here, we discuss the mechanism. First, the questions are summarized as follows: (i)

why is the decomposition rate exceptionally high for the formate prepared from formic acid on O/Cu(111) as well as the decomposition of the synthesized formate in H<sub>2</sub>? and (ii) why was the unique different kinetic behavior observed only for Cu(111)? A possible explanation for the two questions is that the added-row-type reconstruction may occur upon chain formation for all formate species except for the formate prepared from formic acid and O/Cu(111). As mentioned above, on Cu(110), the chain structure of formate has been reported for the formate prepared by adsorption of formic acid on an oxygen-covered Cu(110) surface.<sup>42</sup> The formate chains may be an added-row-type reconstruction such as the well-known (–O–Cu–O–) added rows formed on Cu(110) upon O<sub>2</sub> adsorption. It has been reported that Cu atoms at the step edges are removed and transported onto the terrace to create the –O–Cu–O– added chain on Cu(110).<sup>43</sup> This kind of mass transport may occur in the formation of the formate chain on Cu(111) because the corrugation of the STM image for the synthesized formate (10–20 Å) was much greater than that for the formate prepared from formic acid on O/Cu(111) (1–4 Å). As for the formate prepared from formic acid on clean Cu(111), the corrugation was also high (10–20 Å). This is inconsistent with the same character of the decomposition kinetics, the IRAS intensity and the peak shift between the synthesized formate and the formate prepared from formic acid on the clean Cu(111) surface. The substrate copper atom on Cu(111) might easily migrate by reacting with hydrogen atoms in the presence of high-pressure H<sub>2</sub>, leading to a stable added-row-type formate chain. That is, the driving force to create the formate chain different from the structure of formate prepared by formic acid on O/Cu(111) is related to the presence of adsorbed hydrogen in equilibrium with high-pressure H<sub>2</sub> gas (380 Torr). The (111) planes of Cu are the most stable compared to the other planes; therefore, the surface copper atoms required for the added-row formation would hardly migrate in the absence of adsorbed hydrogen atoms. In the presence of high-pressure H<sub>2</sub> gas, adsorbed hydrogen probably breaks the added-row chain by reacting with Cu atoms. It is thus possible that the attractive interaction between nearest neighbor formate species is vanished and the decomposition rate becomes the same value as the formate prepared from formic acid on O/Cu(111).

**4.4. Comparison with Cu/SiO<sub>2</sub> Powder Catalyst.** We have reported the synthesis and decomposition of formate on a Cu/SiO<sub>2</sub> powder catalyst.<sup>18</sup> The apparent activation energy of the formate synthesis on Cu/SiO<sub>2</sub> was 58.8 kJ mol<sup>-1</sup>, which was comparable with those obtained for Cu(111), Cu(110), and Cu(100) as described in section 3.1. As for the decomposition, the activation energy and preexponential factor for Cu/SiO<sub>2</sub> were 115.7 kJ mol<sup>-1</sup> and 5.38 × 10<sup>-11</sup> s<sup>-1</sup>, respectively. These values were in good agreement with those obtained for Cu(111) rather than Cu(110) and Cu(100). Thus, the surface of Cu particles in the Cu/SiO<sub>2</sub> powder catalyst is expected to comprise the most densely packed Cu(111) plane. Furthermore, the promotion effect of hydrogen in the formate decomposition was also observed on the Cu/SiO<sub>2</sub> powder catalyst.<sup>18</sup> The promotion curve measured for Cu/SiO<sub>2</sub> was very similar to that for Cu(111) shown in Figure 10. It is thus concluded that the Cu(111) surface can be regarded as a model of the Cu/SiO<sub>2</sub> powder catalyst.

## 5. Conclusions

From this work we draw the following conclusions. (1) The formate synthesis on copper at 1 atm is structure-insensitive in terms of the absolute formation rate as well as the activation energy. (2) The kinetics of formate synthesis is consistent with

an Eley–Rideal type mechanism in which an adsorbed hydrogen reacts with a gaseous CO<sub>2</sub> molecule. (3) The decomposition of formate on copper in UHV is structure-sensitive in contrast to the formate synthesis. (4) Measured coverage of formate on Cu(111) and Cu(110) in equilibrium with 1 atm of CO<sub>2</sub>/H<sub>2</sub> is in good agreement with that calculated by the kinetics of the formate synthesis and the formate decomposition. (5) The decomposition kinetics of formate on Cu(111) uniquely depend on the preparation method or the coexistence of H<sub>2</sub>, where the preexponential factor of the rate constant is increased only while the activation energy was identical. The difference in the decomposition kinetics is probably due to the surface structure of formate, diffusion of Cu atoms, or H-induced reconstructing of Cu(111). (6) The selectivity to form a chain or nonchain structure is probably controlled by the mass transport of Cu atoms at the step edges, which is further thermodynamically controlled by temperature and coexisting adsorbates. (7) The Cu(111) surface can be regarded as a model of a Cu/SiO<sub>2</sub> powder catalyst in terms of the kinetics of formate synthesis, formate decomposition, and the unique character of the promotion on the formate decomposition.

**Acknowledgment.** This research was supported by the Grant-in Aid for Scientific Research on Priority Areas “Molecular Physical Chemistry” from the Ministry of Education, Science, Sports, and Culture.

## References and Notes

- Rodriguez, J. A.; Goodman, D. V. *Surf. Sci. Rep.* **1991**, *14*, 1.
- Campbell, C. T. *Adv. Catal.* **1989**, *36*, 1.
- Nakamura, J.; Nakamura, I.; Uchijima, T.; Kanai, Y.; Watanabe, T.; Saito, M.; Fujitani, T. *Catal. Lett.* **1995**, *31*, 325.
- Fujitani, T.; Nakamura, I.; Watanabe, T.; Uchijima, T.; Nakamura, J. *Catal. Lett.* **1995**, *35*, 297.
- Nakamura, J.; Nakamura, I.; Uchijima, T.; Kanai, Y.; Watanabe, T.; Saito, M.; Fujitani, T. *J. Catal.* **1996**, *160*, 65.
- Nakamura, J.; Kushida, Y.; Choi, Y.; Uchijima, T.; Fujitani, T. *J. Vac. Sci. Technol.* **1997**, *A15*, 1568.
- Nakamura, I.; Nakano, H.; Fujitani, T.; Uchijima, T.; Nakamura, J. *J. Vac. Sci. Technol.* **1999**, *A17*, 1592.
- Nakamura, J.; Nakamura, I.; Uchijima, T.; Watanabe, T.; Fujitani, T. *Studies Surf. Sci. Catal.* **1996**, *101*, 1389.
- Nakamura, I.; Nakano, H.; Fujitani, T.; Uchijima, T.; Nakamura, J. *Surf. Sci.* **1998**, *402–404*, 92.
- Nishimura, H.; Yatsu, T.; Fujitani, T.; Uchijima, T.; Nakamura, J. *J. Mol. Catal.* **2000**, *A155*, 3.
- Fujitani, T.; Nakamura, I.; Uchijima, T.; Nakamura, J. *Surf. Sci.* **1997**, *383*, 285.
- Nakamura, I.; Fujitani, T.; Uchijima, T.; Nakamura, J. *Surf. Sci.* **1998**, *400*, 387.
- Fujitani, T.; Choi, Y.; Sano, M.; Kushida, Y.; Nakamura, J. *J. Phys. Chem. B* **2000**, *104*, 1235.
- Fujitani, T.; Nakamura, I.; Ueno, S.; Uchijima, T.; Nakamura, J. *Appl. Surf. Sci.* **1997**, *121/122*, 583.
- Nakamura, J.; Uchijima, T.; Kanai, Y.; Fujitani, T. *Catal. Today* **1996**, *28*, 223.
- Nakamura, I.; Fujitani, T.; Uchijima, T.; Nakamura, J. *J. Vac. Sci. Technol.* **1996**, *A14*, 1464.
- Nakamura, J.; Nakamura, I.; Uchijima, T.; Watanabe, T.; Fujitani, T. *11th Int. Congr. Catal. Stud. Surf. Sci. Catal.* **1996**, *101*, 1389.
- Yatsu, T.; Nishimura, H.; Fujitani, T.; Nakamura, J. *J. Catal.* **2000**, *191*, 423.
- Fujitani, T.; Nakamura, J. *Appl. Catal.* **2000**, *A 191*, 111.
- Taylor, P. A.; Rasmussen, P. B.; Ovesen, C. V.; Stoltze, P.; Chorkendorff, I. *Surf. Sci.* **1992**, *261*, 191.
- Chorkendorff, I.; Taylor, P.; Rasmussen, P. B. *J. Vac. Sci. Technol.* **1992**, *A10*, 2277.
- Taylor, P. A.; Rasmussen, P. B.; Chorkendorff, I. *J. Chem. Soc. Faraday Trans.* **1995**, *91*, 1267.
- Bowker, M.; Rowbotham, E.; Leibsle, F. M.; Haq, S. *Surf. Sci.* **1996**, *349*, 97.
- Leibsle, F. M.; Haq, S.; Frederick, B. G.; Bowker, M.; Richardson, N. V. *Surf. Sci.* **1995**, *345*, L1175.
- Leibsle, F. M. *Surf. Sci.* **1998**, *401*, 153.

- (26) Hayden, B. E.; Prince, K.; Woodruff, D. P.; Bradshaw, M. A. *Surf. Sci.* **1983**, *133*, 589.
- (27) Sexton, B. A.; Hughes, A. E.; Avery, N. R. *Surf. Sci.* **1985**, *155*, 366.
- (28) Dubois, L. H.; Ellis, T. H.; Zegarski, B. R.; Kevan, S. D. *Surf. Sci.* **1986**, *172*, 385.
- (29) Crapper, M. D.; Riley, C. E.; Woodruff, D. P.; Puschmann, A.; Haase, J. *Surf. Sci.* **1986**, *171*, 1.
- (30) Sotiropoulos, A.; Milligan, P. K.; Cowie, B. C. C.; Kadodwala, M. *Surf. Sci.* **2000**, *444*, 52.
- (31) Crapper, M. D.; Riley, C. E.; Woodruff, D. P. *Surf. Sci.* **1997**, *184*, 121.
- (32) Woodruff, D. P.; McConville, C. F.; Kileoyne, A. L. D.; Lindner, T.; Somers, J.; Surman, M. *Surf. Sci.* **1988**, *201*, 228.
- (33) Campbell, J. M.; Campbell, C. T. *Surf. Sci.* **1991**, *259*, 1.
- (34) Anger, G.; Winkler, A.; Rendulic, K. D. *Surf. Sci.* **1989**, *220*, 1.
- (35) Rasmussen, P. B.; Taylor, P. A.; Chorkendorff, I. *Surf. Sci.* **1992**, *269/270*, 352.
- (36) Ying, D. H. S.; Madix, R. J. *J. Catal.* **1980**, *61*, 48.
- (37) Beguin, B.; Denise, B.; Sneed, R. P. A. *J. Organo. Chem.* **1981**, *208*, C18.
- (38) Burgemeister, T.; Kastner, F.; Leitner, W. *Angew. Chem. Int. Ed. Engl.* **1993**, *32*, 739.
- (39) Bianchini, C.; Ghilardi, C. A.; Meli, A.; Midollini, S.; Orlandini, A. *Inorg. Chem.* **1985**, *24*, 924.
- (40) Sakaki, S.; Ohkubo, K. *Inorg. Chem.* **1989**, *28*, 2583.
- (41) Sakaki, S.; Musashi, Y.; *J. Chem. Dalton Trans.* **1994**, 3047.
- (42) Haq, S.; Leibsle, F. M. *Surf. Sci.* **1997**, *375*, 81.
- (43) Jensen, F.; Besenbacher, F.; Legsgard, E. L.; Stensgaard, I. *Phys. Rev.* **1990**, *B 41*, 10233.
- (44) Sexton, B. A. *Surf. Sci.* **1979**, *88*, 319.
- (45) Bowker, M.; Haq, S.; Holroyd, R.; Parlett, P. M.; Poulston, S.; Richardson, N. *J. Chem. Soc., Faraday Trans.* **1996**, *92*, 4683.
- (46) Li, Y.; Bowker, M. *Surf. Sci.* **1993**, *285*, 219.
- (47) Jones, A. H.; Poulston, S.; Bennett, R. A.; Bowker, M. *Surf. Sci.* **1997**, *380*, 31.
- (48) Stone, P. S.; Poulston, S.; Bennett, R. A.; Price, N. J.; Bowker, M. *Surf. Sci.* **1998**, *418*, 71.